Chapter 4
Barriers Preventing the Release of Fission Products

4.1 First Barrier: the Nuclear Fuel Matrix

The nuclear fuel most commonly used in NPPs is ceramic UO_2 pellets with different levels of ^{235}U enrichment. In comparison with other fuel materials, this matrix releases a low rate of fission product.

4.1.1 Properties of UO_2 Nuclear Fuel

A deep knowledge of the properties of the nuclear fuel employed is essential for reliable behaviour during plant operation. The most important properties of UO_2 that are affected by production technologies are:

- enrichment of the fissionable additives (^{235}U, ^{239}Pu, ^{241}Pu);
- chemical purity and stoichiometric coefficients (for example the purity, and the need for $F < 10$ ppm, $H_2 < 1$ ppm, *etc.*);
- density, microstructure, plasticity;
- exact geometrical features (for example the pellet diameter is ≤ 0.013).

These properties depend on how the fuel material is manufactured. Each technological step can influence the properties. There are many ways to obtain uranium dioxide for use as the basic material in ceramic nuclear fuel. The most common are:

- reduction of UO_3 obtained from the uranylnitrate;
- ammonium diuranate (ADU) reduction;
- oxidation of uranium in a water bath or in water vapour;
- reduction of U_3O_8;
- direct conversion of UF_6.

In the following steps, the UO_2 is passed through a granulation process. There are only two technologies that can be applied here. In the wet granulation process, a soft UO_2 powder is processed with binders. Then it is precompacted, dried, broken, and

pressed with lubricants. The other possibility is a dry granulation process, where UO_2 is cold pressed, broken again, mixed with lubricants, and pressed.

The options for pelletizing include:

- cold pressing in the die and sintering;
- warm isostatic pressing;
- extrusion pressing and sintering (warm, cold);
- tempering, pressing and sintering;
- swaging;
- vibration compacting in the die;
- high-energy forming;
- tandem rolling.

A pressure of 1–5 t/cm^2 (100–500 MPa) is used during pressing, and the content of lubrication oils cannot exceed 0.5 weight%. The sintering process is done in an H_2, H_2/N_2 or $H_2 + CO_2$ atmosphere. Afterwards, the surface is ground and the cylinder-like UO_2 can be used in the pile.

4.1.1.1 Sintering Technology

Sintering is a process in which a compact of a crystalline or non-crystalline powder is heat-treated to form a single, coherent solid. In general, three types of sintering processes are important to the production of ceramics:

- *Vitrification* – heat treatment which produces enough viscous liquid at the firing temperature to completely fill the porous spaces in the original powder compact. This process is relatively inexpensive and is of particular importance in the production of porcelain and clay-based ceramics.
- *Liquid-phase sintering* – the composition is such that enough liquid forms at the firing temperature to allow easy rearrangement of the particles, but not enough to fill the initial porosity; subsequent solution and re-precipitation of the solid in the liquid phase then allows the particles to be reshaped and a dense body is formed. This method is often effective and reasonably inexpensive, but the resulting grain boundary phase may be detrimental to high-temperature mechanical properties (*e.g.*, creep resistance).
- *Solid-state sintering* – all constituents of the compact remain solid during the entire process; all densification is achieved by changing the grain shape. Sintering aids that will not form a liquid may be added in amounts ranging from a few hundred parts per million to over 20%. This method is preferred for the production of technical ceramics (*e.g.*, nuclear fuel pellets) with good mechanical, electronic or optical properties, particularly when optimal high-temperature properties are required [2, 3].

The important variables in the sintering process are:

- the processing temperature;
- the time spent at each stage of the process;

- the particle size and the size distribution of the ceramic powder;
- the composition of the system, including additives and atmosphere;
- the processing pressure applied when hot pressing or a controlled atmosphere is used.

Obviously, this work is concerned with solid-state sintering, because it considers the nuclear field, especially the properties of fuel pellets.

4.1.1.2 The Driving Force for Sintering

The primary driving force for sintering is a reduction in the free surface energy of the system. This is accomplished by reducing the area of the surfaces and interfaces of the compact, which can be achieved by a combination of two processes that occur simultaneously during the sintering of a ceramic powder compact: *densification* and *coarsening* (grain growth) [2, 4]. Densification is the process of replacing the free surface energy with grain boundary energy, while coarsening involves reducing the free surface or grain boundary energy. Thus, the microstructural changes that occur during sintering are brought about by the combined effects of coarsening and densification processes. The relative contributions of these two subprocesses depend on the processing variables: temperature, time, composition and particle size.

The driving force for sintering (a reduction in excess surface free energy) is translated into a driving force that acts at the atomic level (thus resulting in atomic diffusion) by means of differences in curvature that inherently occur in different parts of the three-dimensional compact. These differences in curvature create chemical potential and vacancy concentration differences, and thus control the direction of matter transport. The relationship that links surface energy, curvature and concentration differences is the Gibbs–Thomson equation:

$$C(r) = C_\infty \exp\left\{\frac{2\gamma\Omega}{r k_\mathrm{B} T}\right\} , \tag{4.1}$$

where:

$C(r)$ is the vacancy concentration under a surface which has a radius of curvature $\boldsymbol{r}$;
C_∞ is the vacancy concentration under a plane;
γ is the surface energy;
Ω is the volume occupied by a vacancy;
k_B is the Boltzmann constant;
T is the temperature.

The Gibbs–Thomson equation applies to concentrations of dilute species and is therefore applied to vacancies which are in dilute solution in the solid rather than to the atoms themselves. Once the flow equations are known in terms of the vacancies, the equivalent flow in terms of atoms follows directly.

In the powder compact, the vacancy concentration will be different in regions with different curvatures, resulting in vacancy gradients and thus vacancy flow. The rate of mass transport is described by Fick's first law of diffusion:

$$J = -D\frac{\mathrm{d}c}{\mathrm{d}x}\,, \tag{4.2}$$

where:

J is the vacancy flux;
D is the vacancy diffusion coefficient;
$\mathrm{d}c/\mathrm{d}x$ is the concentration gradient.

During the initial stages of sintering, there will be a net flow of vacancies from the neck that forms between particles. This flow of vacancies is exactly equivalent to a flow of atoms in the opposite direction, thus resulting in neck formation.

It is often helpful in the case of ceramics to consider an alternative representation of the driving force for atom movement. In this representation, a flow of atoms stems from the normal pressure differences which occur in regions of the solid close to surfaces with different curvatures. This representation leads to a diffusion flux which can be written as:

$$J = -\frac{D}{k_\mathrm{B}T}\frac{\mathrm{d}P}{\mathrm{d}x}\,, \tag{4.3}$$

where:

J is the vacancy flux;
D is the vacancy diffusion coefficient;
k_B is the Boltzmann constant;
T is the temperature;
$\mathrm{d}P/\mathrm{d}x$ is the pressure gradient.

Surface energy forces create regions with different pressures under different curvatures. Atoms will tend to flow from regions of high pressure to regions of low pressure. This concept avoids the need to rely on atom movements due to vacancies; it therefore also applies to systems in which atoms move by other defect mechanisms.

This approach that links atom movement to pressure differences has the benefit of directly describing the diffusive deformation of dense polycrystalline materials caused by an applied stress (creep). Sintering rate equations for ceramics have been developed according to the assumption that behaviour caused by pressure differences during sintering is similar to diffusion creep behaviour. The rate of deformation caused by an applied stress is given by the general equation:

$$\varepsilon = \frac{AD}{k_\mathrm{B}T}\left(\frac{b}{G}\right)^m\left(\frac{\sigma}{g}\right)^n\,, \tag{4.4}$$

where:

ε is the rate of deformation;
A is the dimensionless constant;

D is the appropriate diffusion coefficient;
k_B is the Boltzmann constant;
T is the temperature;
g is the shear modulus;
b is the magnitude of the Burgers vector;
G is the grain size;
σ is the applied stress;
m, n are constants that depend upon the transport mechanism.

Low temperature (in relation to the melting point of the material) creep of metals is usually controlled by dislocation movements, because their structures contain sufficient active slip systems and have small Peierls stresses (the force needed to bring about dislocation movement) [4–8]. Deformation can also be controlled by dislocation climb, a process requiring vacancy diffusion. At high temperatures, deformation in metals is usually controlled by diffusion creep mechanisms that do not involve dislocation movement. In ceramics, however, diffusion creep may be the dominant mechanism under most processing conditions due to the small number of slip planes, the high Peierls stresses, and to the need to move stoichiometric amounts of the different atomic species present in the material (both anions and cations for an ionic compound).

4.1.1.3 Stages of Sintering

Investigations of sintering behaviour have commonly been simplified by assuming that the densification takes place in stages. The sintering process is usually modelled with three stages:

- *initial* – the individual particles of the green compact, which remain readily identifiable, are bonded together by neck growth between the particles, and grain boundaries form at the junctions between particles;
- *intermediate* – characterised by interconnected networks of particles and pores;
- *final* – the structure is composed of space-filling polyhedral and isolated pores.

There are no clear-cut divisions between the three stages. During the initial stage, the individual particles of the green compact, which remain readily identifiable, are bonded together by the growth of necks between the particles, and a grain boundary forms at each junction between two particles. The initial stage ends when the growing necks begin to impinge on each other, or at $\sim 5\%$ shrinkage.

4.1.2 Grain Growth

The reduction in the free surface energy of the system is achieved by reducing the surface area by one or a combination of the following three processes:

- replacing the gas/solid interfaces with lower energy solid/solid interfaces (densification);
- converting many small particles into fewer large ones (coarsening); and/or
- reducing the grain boundary area through grain growth (coarsening).

Grain growth means increasing the grain size in a single-phase material or the matrix grain size in a material with second-phase particles. The sum of the individual grain sizes is constant, and the increase in average grain size is thus due to the disappearance of some of the grains, usually the smaller ones. In practice, one distinguishes between *normal* or *continuous* grain growth and *abnormal* or *discontinuous* grain growth [6]. During normal grain growth, the individual grains are relatively uniform in size. However, during abnormal grain growth, some of the grains grow more rapidly than the others. When they have consumed all of the other grains, the remaining grains may again be relatively uniform in size. Large grains are desirable because less fission gas is released from a nuclear fuel with large grains during irradiation, they permit higher discharge burnup, and using large grains reduce the amount of irradiated fuel that needs to be stored and reprocessed [5].

4.1.2.1 Methods of Producing a Large Grain Structure in UO_2

Methods that can be used to produce a large grain structure in UO_2 can be divided into the following categories [5]:

- purely thermal treatment of the UO_2;
- modifying diffusion coefficients by changing the stoichiometry;
- chemical methods, which generally involve the use of additives.

UO_2 pellets are commonly sintered in hydrogen at 1770 °C for periods of about 4 h. At the end of this period, the grain size is typically about 10 µm. If the sintering is prolonged, the grain size will increase but at a diminishing rate, since the rate of grain growth is related to the grain size by

$$\frac{\mathrm{d}D}{\mathrm{d}t} = \frac{k}{D^n} \tag{4.5}$$

and

$$k = k_0 \exp\left(-\frac{E}{RT}\right) , \tag{4.6}$$

where:

$\mathrm{d}D/\mathrm{d}t$ is the grain growth rate;
D is the grain size;
E is the activation energy;
R is the gas constant;
T is the temperature;
k_0 is a constant;
n is another constant; it usually has a value somewhere between 1 and 2.

Grain growth occurs at all stages of the sintering process. Most theories and models of grain growth consider coarsening only during the final stage of sintering, as the primary goal of the sintering of ceramics is to achieve high density while maintaining a fine, uniform grain size, and most ceramics that sinter well do not undergo excessive grain growth until nearly full density is reached.

The simplest model of grain growth considers the movement of a single grain boundary in a pure, dense material. There is a free energy difference ΔG across a curved grain boundary:

$$\Delta G = \gamma V_{\mathrm{m}} \left(\frac{1}{r_1} + \frac{1}{r_2} \right) , \tag{4.7}$$

where:

ΔG is the difference in free energy;
r_1, r_2 are the principal radii of curvature;
γ is the surface energy;
V_{m} is the molar volume of atoms moving across the boundary.

This free energy difference provides the driving force for the boundary to move towards its centre of curvature. The rate of boundary movement is proportional to the curvature, and thus inversely proportional to the average grain size and proportional to the ability of the atoms to cross the grain boundary. The rate of grain growth is then:

$$\frac{\mathrm{d}G}{\mathrm{d}t} \approx \frac{D^*_{\mathrm{gb}}}{\overline{G}} , \tag{4.8}$$

where:

$\mathrm{d}G/\mathrm{d}t$ is the rate of grain growth;
D^*_{gb} is the grain boundary;
$\overline{G}$ is the average grain size.

Soluble impurities can segregate towards or away from a grain boundary, provided the resulting effect is to reduce the free energy of the system. There is a complex relationship between the velocity of a grain boundary, the diffusivity of the impurity, and the interaction of the impurity with the grain boundary. Qualitatively, at high boundary velocities, faster-diffusing impurities will exert the greatest drag. At low velocities, slower-diffusing impurities will cause the greatest drag. In the high-velocity case, only the fast-diffusing atoms can remain at the boundary and affect its mobility. In the low-velocity case, the fast-diffusing atoms will be able to redistribute themselves quickly enough to maintain the lowest energy distribution, while the slower diffusing atoms will obstruct boundary movement. Increasing the impurity concentration or decreasing the temperature will change the diffusive behaviour and thus increase the drag effect of the impurity [9–12, 16].

The low-velocity case, which is thought to be applicable to normal grain growth in single-phase ceramics, has been examined. In this case, the boundary velocity can

be written as:

$$v_{\mathrm{b}} = F_{\mathrm{b}} \left(\frac{M_{\mathrm{b}}}{1 + M_{\mathrm{b}} \alpha C_{\mathrm{o}}} \right) , \tag{4.9}$$

where:

F_{b} is the driving force;
M_{b} is the boundary mobility;
C_{o} is the bulk impurity concentration;
α is the drag force on the grain boundary for unit volume and unit concentration when the boundary velocity or solute diffusion time is small.

Second-phase particles or other inclusions in the microstructure will also inhibit grain growth. As a grain boundary moves past a particle, the area of the boundary is reduced by an amount equal to the cross-sectional area of the particle. The surface area, and the surface energy, must increase if the boundary is to pull away from the particle. The particle thus exerts a restraining force on the grain boundary of

$$F_{\mathrm{max}} = \pi r \gamma_{\mathrm{gb}} . \tag{4.10}$$

The grain growth is then:

$$\frac{\mathrm{d}G}{\mathrm{d}t} = F_{\mathrm{b}} - F_{\mathrm{p}} \approx \frac{D^{*}_{\mathrm{gb}}}{G} - \pi G \gamma , \tag{4.11}$$

where:

F_{b} is the force on a curved boundary;
F_{p} is the maximum drag force of a particle;
γ is the surface energy of the grain boundary.

If there are a number of inclusions at the boundary, the boundary driving force may be insufficient to move it past the inclusions. The grain size limit in this case is:

$$G_{\mathrm{lim}} \cong \frac{3a}{4V_{\mathrm{v}}} , \tag{4.12}$$

where:

G_{lim} is the grain size limit;
a is the radius of each randomly dispersed spherical particle;
V_{v} is the volume fraction.

Pores can behave much like inclusions in retarding grain boundary movement. However, the situation is more complex since – unlike most inclusions – pores can move by diffusion. Pores move by transferring atoms from the front of the pore to the back. This transfer can take place by any of the diffusion mechanisms with a surface source. The effect of a pore on boundary movement will depend upon its mobility relative to that of the boundary and the geometry of the system [13, 15].

For simplicity, pores are often modelled as being spherical; however, the pore cannot actually be spherical if there is a driving force for diffusion. The pores can remain attached to the moving boundary if the velocities of the pore and the boundary are equal:

$$v_{\mathrm{p}} = v_{\mathrm{b}} \tag{4.13}$$

and

$$v_{\mathrm{b}} = NF_{\mathrm{p}} + \frac{M_{\mathrm{p}}F_{\mathrm{p}}}{M_{\mathrm{b}}}\ , \tag{4.14}$$

where:

v_{p} is the velocity of the pore;
v_{b} is the velocity of the boundary;
N is the pore density at the boundary;
M_{p} is the mobility of the pore;
M_{b} is the mobility of a pore-free boundary;
F_{p} is the maximum force exerted on the boundary by the pore.

The boundary and pore separate if:

$$v_{\mathrm{p}} = F_{\mathrm{p}}M_{\mathrm{p}} < v_{\mathrm{b}} = \left(F_{\mathrm{b}} - NF_{\mathrm{p}}\right) M_{\mathrm{b}} \tag{4.15}$$

or

$$F_{\mathrm{b}} > NF_{\mathrm{p}} + \frac{M_{\mathrm{p}}F_{\mathrm{p}}}{M_{\mathrm{b}}}\ . \tag{4.16}$$

Small pores can move faster than large pores [14]. Many large pores will exert a large restraining force on a boundary. During the early portion of the final stage of sintering, both the grains and the pores are small. These small pores will not exert much drag on the boundary unless there are many of them. Whether the pores remain attached or not will depend on the relative velocities of the pores and boundary [15, 17].

During the later stages of sintering some grains may grow to be much larger than the average grain size if conditions are favourable, often trapping pores within the grain, resulting in a reduced final density. These large grains may also reduce the strength of the material by acting as stress concentrators. A large grain surrounded by small grains will have many grain boundaries, each with a small, convex (from the perspective of the large grain) radius of curvature. Each of these boundaries will have a high driving force, causing it to move away from the large grain, thus further increasing the size of the grain and promoting further growth. Milled powders often have a few very large grains that may grow abnormally. Such growth can also occur in regions with fewer than average second-phase particles or low solute concentrations, and is very likely to occur when pores become so small that they no longer restrain boundary movement. Density variations in a sample may lead to a wide grain size distribution, allowing abnormal grain growth [5, 6, 18–21].

4.2 Second Barrier: Fuel Cladding

The fuel cladding is the second barrier, and (from the viewpoint of normal operation) the most significant barrier preventing the release of fission products into the reactor coolant. Regular and proper leak testing of fuel assemblies is an inevitable requirement that is closely related to not only operational regulations but also attempts to assure optimal operation from a radiation protection point of view.

4.2.1 Leakage Monitoring Techniques for VVER-440 Reactors

In the core of a nuclear reactor, a wide variety of radionuclides are produced as a result of fission and activation processes. The fuel cladding is the most important protective barrier that prevents the release of most of the fission products from the fuel matrix into the coolant. The walls of the primary circuit serve as the next protective barrier that prevents the movement of radionuclides from the primary to the secondary circuit. When the cladding fails the coolant interacts with the fuel; fission products migrate – depending on their volatilities – into the coolant through "tight" defects, while fuel fragments may also get into the primary coolant if there are "open" defects in the cladding. Because of their multiple protection systems, nuclear reactors can be and often are operated in the presence of a certain number of defective fuel elements, but safety aspects and the long-term effects of contamination must be taken into account. There is also an economic limit on operating with failed fuels, bearing in mind the safety limit set by the nuclear regulatory authority. Monitoring fuel performance is an especially important task when the fuel policy of the reactor permits operation in the presence of defective fuels [22–24].

By monitoring the activity concentrations of several short-lived radionuclides (*e.g.*, iodine and noble gases) in the primary coolant, fuel defects can be identified, and the defect type (tight or open) and number of leaking elements can be assessed. Major nuclear characteristics of the defective element, such as burn-up and the original ^{235}U enrichment, can be determined by measuring the activity ratios of certain long-lived nuclides (*e.g.*, cesium, transuranium), so failed elements can be localised.

The concentrations of the radionuclides originating from both the uranium concentration of the core and defective fuels are measured regularly. Iodine and cesium nuclides are measured by gamma spectroscopy. Occasionally, alpha and beta spectrometric analyses are performed to determine transuranium and strontium isotopes, respectively.

Fuel leakages are qualitatively indicated by a sudden increase in the concentrations (spiking) of fission products, especially noble gases and iodine nuclides. The appearance of less volatile nuclides in the coolant (*e.g.*, transuranium nuclides) suggests the occurrence of open defects.

The following mathematical approaches can be used for quantitative fuel characterisation.

4.2.1.1 Surface Contamination

It is assumed that the shortest-lived iodine isotope, ^{134}I, originates only from surface contamination of the reactor core. Thus, the amount of transuranium is calculated from the ^{134}I concentration.

4.2.1.2 Defect Type

Two major types of defect can be distinguished without the need to define their sizes exactly: *tight* and *open*. Tight defects allow mostly volatile fission products to migrate into the coolant after some retention, while open defects also permit the release of fuel fragments into the water. Two release mechanisms can be distinguished:

- Releases from tight defects are characterised by a high ^{131}I to ^{133}I concentration ratio, assuming the preferential accumulation of the longer-lived nuclide in the fuel element;
- Releases from open defects are characterised by a low concentration ratio of ^{131}I to ^{133}I, assuming the relatively free leakage of all iodine nuclides.

The leak model can be determined by applying a criterion, the ratio of the corrected activity concentrations (A_{corr}) of ^{131}I and ^{133}I, where the actual concentrations of the longer-lived iodine nuclides (^{131}I and ^{133}I) are corrected for surface contamination according to the following equations:

$$A_{\text{corr}}^{\text{I-131}} = A_{\text{meas}}^{\text{I-131}} - A_{\text{bg}}^{\text{I-131}} \tag{4.17}$$

$$A_{\text{bg}}^{\text{I-131}} = K^{\text{I-131}} . A_{\text{meas}}^{\text{I-134}} \tag{4.18}$$

$$K^{\text{I-131}} = \frac{\frac{\lambda^{\text{I-131}} . Y^{\text{I-131}}}{\lambda^{\text{I-131}} + \beta}}{\frac{\lambda^{\text{I-134}} . Y^{\text{I-134}}}{\lambda^{\text{I-134}} + \beta}} , \tag{4.19}$$

where:

λ is the decay constant (s^{-1});
β is the cleanup rate of the water cleanup system (s^{-1});
Y is the fission yield (no units).

The following criteria are applied. There are fuel elements with tight defects in the core if

$$\frac{A_{\text{corr}}^{\text{I-131}}}{A_{\text{corr}}^{\text{I-133}}} \geq 0.7 . \tag{4.20}$$

There are fuel elements with open defects in the core if

$$0.2 < \frac{A_{\text{corr}}^{\text{I-131}}}{A_{\text{corr}}^{\text{I-133}}} < 0.7 . \tag{4.21}$$

Finally, there are no defective elements in the core if

$$\frac{A_{\text{corr}}^{\text{I-131}}}{A_{\text{corr}}^{\text{I-133}}} \leq 0.2 \; . \tag{4.22}$$

4.2.1.3 Number of Defective Fuel Elements

The number of defective fuel elements can be calculated by dividing the corrected iodine ^{131}I activity concentration ($A_{\text{corr, I-131}}$) by the concentration of the same nuclide observed with a standard leak ($A_{\text{i, st}}$).

4.2.1.4 Localisation of Defective Fuel Elements

Fuel burnup can be determined by measuring the activity ratios of radionuclides with long half-lives. Assuming that the ratios of the nuclides in the fuel are equal to those in the coolant, the burnup level of the defective fuel can be estimated. By measuring the ^{137}Cs/^{134}Cs, ^{238}Pu/^{239,240}Pu and ^{244}Cm/^{239,240}Pu ratios in the coolant and comparing those values with the calculated ones for a certain reactor, the burnup of the defective element can be calculated. Since transuranium nuclides are released only through defects, their activity ratios provide information about the burnup of badly damaged fuel, while cesium ratios are characteristic of all types of failed elements and are more generally used for localisation purposes.

Reliable identification of damaged fuel assemblies is only possible during refuelling outages. Nevertheless, all of the methods mentioned above can aid in the early identification of leakages in the fuel rod cladding.

4.2.2 Leak-testing Performance at the Bohunice NPP

Until 1986, all fuel sipping tests were performed using a Soviet wet canister pool system. During refueling outages, several fuel assemblies were tested. This type of leak testing equipment was not optimal, mainly because of the long testing time.

In 1986, in-core sipping equipment designed and manufactured by Siemens KWU was purchased [22, 23]. Since then, full core sipping tests have been performed in all cases where the occurrence of a leak has been demonstrated by operational data. The decision to perform sipping tests was taken based on primary coolant activity measurements obtained during reactor operation and iodine spike analysis.

The extent to which fission products are released from the fuel rods to the coolant inside the channel is dependent on the increase in the temperature of the fuel. During leak testing, the flow of coolant through the assembly is throttled by blocking its upper end. The decay heat produces a rise in the temperature of the fuel and thus

a subsequent increase in the amount of fission gas released. The temperature effect observed in the sipping tests causes an increase in the free gas volume (by up to 3%).

In a defective rod, the fission gases expand and escape through the leak into the surrounding water. The resulting increase in fission product activity can be measured in water samples taken from the assembly. These samples are analysed using a germanium detector. The nuclides ^{134}Cs, ^{137}Cs, ^{131}I and ^{133}Xe are used to identify leaking assemblies. These fission products are either produced directly during reactor operation or as daughter nuclides of short-lived fission products. Their half-lives are long enough to allow them to be detected shortly after reactor shutdown or even after long storage periods (via cesium isotopes).

The in-core sipping equipment used at the Bohunice NPP was also employed once at the Paks NPP in Hungary (1991) and twice at the Dukovany NPP (1991, 1992) in the Czech Republic.

4.2.3 Occurrence of Leaking Fuel Assemblies and Probable Causes of Leaks

Based on in-core sipping test results at Bohunice NPP, 63 leaking fuel assemblies were identified (see Table 4.1).

The fuel failure rate at the SE-EBO NPP (2008) is comparable with fuel failures at other NPPs (see Table 4.2).

The VVER-440 core has hexagonal symmetry. One-sixth of the core matrix was used to display the last in-core position of each leaking fuel assembly. About 25% of all leaking fuel assemblies were located directly in the neighbourhood of the

Table 4.1 Leaking fuel assemblies in Bohunice NPP

	Unit 1	Unit 2	Unit 3	Unit 4
Number of leaking fuel assemblies	17	42	2	2

Table 4.2 Fuel failure rates at various NPPs during the 1980s and 1990s

	Reactor type	Number of reactor units	Typical failure rate in the 1980s and 1990s (a.u.)
Siemens AG	PWR+BWR	30 + 15	1×10^{-5}
Fragema	PWR	50	1.5×10^{-5}
ABB Atom	PWR+BWR	6 + 16	5×10^{-5}
VVER-1000	PWR	19	8×10^{-5}
VVER-440	PWR	28	7×10^{-5}
Paks NPP	PWR	4	5×10^{-5}
Bohunice NPP	PWR	4	4×10^{-5}

power-control assembly. This fraction is unexpectedly high considering the fraction of all fuel assemblies that are in this region – 13% in a full core loading pattern and 15% in a reduced core loading pattern (36 dummies were placed at unit 2 at the core periphery in the Bohunice NPP in 1985). This fact suggests that the PCI mechanism is involved in leak generation; however, the set of 63 fuel leaks is statistically too small to allow any rigorous conclusions to be drawn. Also, Russian reports and experience as well as experience obtained at units 3 and 4 of the Bohunice NPP do not indicate a high probability of a PCI mechanism.

The high number of leaking fuel assemblies at unit 2 of the Bohunice NPP (a total of 42) is also rather interesting. Because of the large number of leaks in one cycle, which faded in subsequent cycles, we can assume that debris-induced fretting was the cause of the leaks. After subtracting the cycles for 1989 and 1990, unit 2 at Bohunice is comparable to unit 1 at Bohunice, or Loviisa 1 and 2. In spite of this, we can assume that leaks occur more frequently at V-230 NPPs than in type V-213 NPPs (as represented by Bohunice 3 and 4, Dukovany 1, 2, 3 and 4, and Paks 1, 2, 3 and 4).

All of the identified leaking fuel assemblies were tested in the Russian canister pool sipping system too. The results of these tests showed that the Russian canister pool sipping system is able to discover leaks.

Some tests showed that, in the case of small leaks, the sensitivities of both methods were comparable, while canister pool sipping provides higher sensitivity for large cladding defects. The main disadvantage of using the canister pool sipping method with a VVER-440 is the time needed, which does not allow for full core testing during refueling. The time needed for canister pool sipping is 14 days, while it is only 48 hours for in-core sipping. However, our experience indicates that the in-core sipping method is currently the best to use for leak testing management from an operational point of view.

4.2.4 The Mast Sipping Method for VVER-440

The mast sipping technique is currently used for many reactor types around the world. For VVER-440s, it was developed and officially registered as an invention in 1991. Unfortunately, there was no interest in using it instead of the well-proven and internationally accepted sipping in-core technology.

4.2.5 The Pool Sipping Method for VVER-440 Fuel at the Wet Interim Burned Fuel Storage at Jaslovské Bohunice

The Interim Spent Fuel Storage Facility (ISFSF) in Jaslovské Bohunice [24, 25] is an important component of the spent nuclear fuel management system. The facility has been used for storage purposes since 1987. ISFSF is a nuclear facility that enables the safe storage of the spent nuclear fuel from VVER-440 reactors for a time

period of 50 years before the fuel is further processed in a reprocessing plant or appropriately disposed of.

It is necessary to keep the concentration of fission products in storage pools at a low level to ensure that the activity of the coolant is acceptable. This can be done by periodically monitoring the condition of each fuel element, identifying defects and enclosing leaking assemblies or fuel elements in special hermetic caskets. This was the main reason for including not only a "sipping in pool" system, but also the SVYP-440 inspection stand (Figure 4.1) in the ISFSF [26, 27].

The sipping in pool system was built and implemented in the storage facility in 1999, and has since provided important results. The system increases the temperature of the fuel assembly (via external heaters), which causes the pressure inside fuel elements to increase. If there is any leakage, this increased pressure will promote fission product release. By measuring the released activity, the assembly leak tightness can be determined.

Since December 2006, the new SVYP-440 stand used for VVER-440 fuel assembly inspection has been operational. Incorporating several modules, it has the ability to open the fuel assembly and take it apart so that all of the fuel elements can be examined. If a defect is found, the fuel element with the defect is enclosed in the special hermetic casing.

Slovakia has more than 20 years of experience with spent fuel storage. No leakages have ever been detected during storage. Even though the negative effects of fuel cladding are very low, there is a finite possibility of defect formation due to the degradation of zirconium alloys after long periods of storage under water. It is also

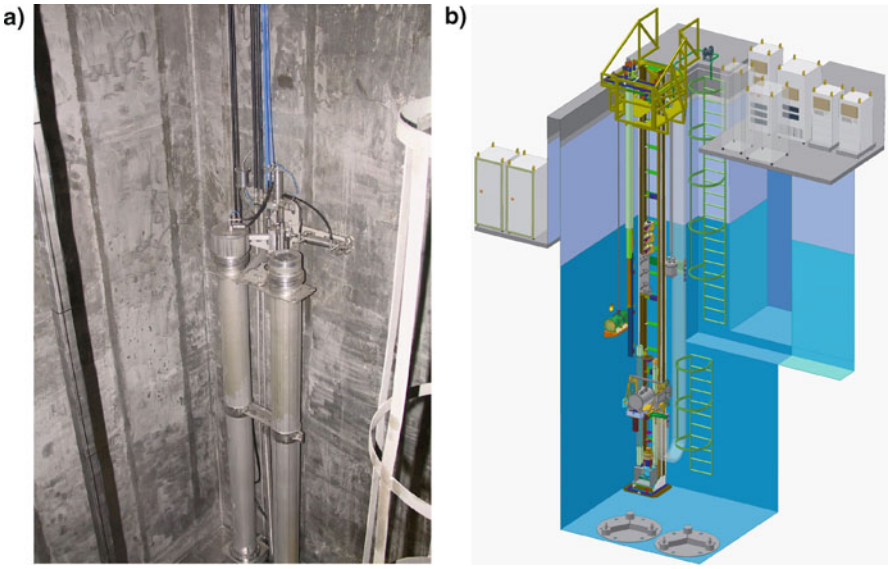

Figure 4.1 Equipment used to monitor and control spent VVER-440 fuel assemblies in Slovakia: **a** sipping in pool, and **b** SVYP-440

http://www.springer.com/978-1-84996-419-7

Safety of VVER-440 Reactors
Barriers Against Fission Products Release
Slugen, V.
2011, XI, 178 p., Hardcover
ISBN: 978-1-84996-419-7